MOLECULAR DYNAMICS SIMULATION OF TRANSPORT OF ENCAPSULATED DRUG THROUGH A LIPID BILAYER

A Thesis Presented to the Department of
Theoretical Physics

African University of Science and Technology
Abuja-Nigeria

In partial Fulfilment of the Requirements
For the Degree of

MASTERS DEGREE IN THEORETICAL PHYSICS

By

Ibrahim Buba Garba

Supervisor:

Dr. Omololu Akin-Ojo.

African University of Science and Technology
www.aust.edu.ng
P.M.B 681, Garki, Abuja F.C.T
Nigeria.

December, 2014

MOLECULAR DYNAMICS SIMULATION OF TRANSPORT OF ENCAPSULATED DRUG THROUGH A LIPID BILAYER

By:
IBRAHIM BUBA GARBA

A THESIS APPROVED BY THE DEPARTMENT OF THEORETICAL PHYSICS

RECOMMENDED:

.....
Supervisor: Dr. Omololu Akin-Ojo

.....
Head, Department of Theoretical Physics

APPROVED:

.....
Chief Academic Officer

.....
Date

Abstract

Most anticancer drugs are polar, cytotoxic and have complicated structures which cause difficulty in their penetration through the cell membrane. This presents a serious problem in chemotherapy. Is it possible to use carbon nanotubes (CNTs) as intracellular drug delivery agents to concomitantly mininmize side effects and maximize therapeutic effect? Although previous experimental and simulation studies have demonstrated that CNTs are able to translocate through cell membrane, the cell penetration mechanisms are not well understood. In this study, we used molecular dynamics simulation to examine the transport of an anticancer drug, Cisplatin, (with and without encapsulation in a CNT) across a solvated DPPC (1,2-DIPALMITOYLPHOSPHATIDYLCHOLINE) lipid bilayer which represents the cell membrane.

Acknowledgements

All praise is due to Allah, peace and blessing be upon the holy prophet Muhammad (S.A.W), his family, his faithful companions and those who follow their footsteps till the day of judgement.

Firstly, I would like to thank my supervisor, Dr. O. Akin-Ojo, a rarity indeed, for his guidance and insight during my research. He made a novice such as me to run a large scale MD simulations. My appreciation also goes to my sponsors BOVAS and Company Limited, NMI and AUST.

I am grateful to my parents, Alh. Garba Buba, Haj. Hasana Hasan and Haj. Amina Ibrahim. Thanks are due to my sisters, Haj. Ruqayyah, Haj. Inna and Haj. Bilkisu, my brothers, Alh. Abubakar, Alh. Muhammadu, Abdul-Muttallib, Auwal, Yahya, Shettima, Lawan, Saddam, Baffale and Gaddafi, my causins, Usman, Saleh and Muhammad.

I would particularly like to thank Dr. Ali Adamu Tikau for his assistance and encouragement.

Finally, I want to thank all of the friends that I've made in AUST over the past 16 months. Specifically, there are nine I would like to thank: Mas-ud, Yusuf, Udoka, Luke, Loreta, Francis, Bruno, J. Asare, and Usman Bello Abdulmalik.

Dedication

I dedicate this work to my parents.

Life should be lived not avoiding problems but welcomig them as challenges that will strict us so that we can be victorious in the future.

Contents

List of Figures

List of Tables

CHAPTER 1

Introduction

"Everything that living things do can be understood in terms of the jigglings and wigglings of atoms"

Richard Feynman

1.1 Overview

Traditional chemotherapy is ineffective and often accompanied by harmful side effects due to the inability of anticancer drugs to discriminate cancer cells from healthy cells. In essence, most anticancer drugs act on rapidly dividing healthy and cancer cells. This drawback can be overcome by Targeted Drug Delivery, where drugs are directed in a site-specific manner to the intended cells thereby minimizing side effects and and enhancing drug concentration in the target sites. The target (receptors) are molecules expressed or overexpressed in cancer cells that are involved in growth, progrssion and spread of cancer cells [3]. Once identified, these receptors can be targeted by small molecules (antigens or peptides called *Molecular Recognition Units MRUs*) that can recognize and bind to them. MRUs that interact with targets/receptors are usually attached to drugs but this often results in complicated strucures that cannot easily permeate cell membrane. Due to their small dimensions, nanoparticles exhibit unique properties (e.g. ability to cross cell membrane) allowing drugs to attach leading to the concept of *magic bullet*. Drug(s) may be adsorbed, covalently linked or encapsulated into the nanoparticles [1].

Different researches have shown that nanocarriers can transport drugs to the place of action, hence increasing accummulation of therapeutic drugs and reducing undesirable side effects. Various nanostructures or *nanovectors*, including liposomes, polymers, dendrimers, silicon and carbon nanomaterials, and magnetic nanoparticles, have been tested as carriers in drug delivery systems [1]. Nanoparticles (NPs) are structures of sizes ranging from 1 to 100nm in at least one dimension[1]. The use of nanoparticles as drug delivery agents is now one of the most active areas of biomedical research both in the academic laboratories and pharmaceutical industires.

Amongst the different nanoparticles (NPs), carbon nanotubes (CNTs), especially single-walled carbon nanotubes (SWCNTs) have attracted tremendous attention owing to their exellent properties. These properties include high surface area, enhanced cellular uptake [13], possibility to be easily conjugated by many molecules [14] leading to superior efficacy, enhanced specificity and diminished side effects. A number of experimental studies have shown that functionalized CNTs can be internalized by a variety of cell types [37] [38] to deliver therapeutic drugs.

Over the years, different experimental groups reported contradicting accounts of the penetration of NPs into cell membrane. Pontaretto et. al. reported that CNT uptake by cells is govern by energy independent non-endocytic pathways that involve diffusion [39]. Chekurai et. al. suggested active uptake of CNTs by macrophages [40]. Another study reported that no single mechanism can be predominanly responsible for celluar uptake of CNTs and that a combination of mechanisms may be the result of their observed cellular uptake [41]. There are several reasons for this ensuing controversy, chiefly among them is the lack of reliable atomic scale insight of the dynamical process from computer simulations. Thus, despite this explosive growth in biomedical application of CNTs, knowledge regarding how they cross cellular barrier remain minimal.

Molecular Dynamics (MD) simulation is a powerful computational tool that can be used to provide this much needed atomistic understanding of the transport process of NPs through the membrane. MD has other uses in the Pharmaceutical industry, for example in drug design. The design of one new drug approved by FDA takes about 15years at the expense of nearly 1 billion USD [1]. In order to shorten this process and make it less expensive, computer simulations are used. Molecular Dynamics (MD) simulation, althought mostly used for the study of structure and key properties like stability, diffusion, binding between molecules and vibration, is nowadays widely used in drug design [2] to accelerate the selection/evaluation process of lead compounds and validate them as potential drugs prior to synthesis and animal studies.

Previous MD studies of drug delivery have mainly focused on encapsulation, self assembly or release mechanisms triggered by optical heating, magnetic field [28], chemical trigger (e.g PH) [29], competetive replacement and enzymatic degradation [30].
Motivated by recent experimental results on the internalization of CNT-encapsulted Cis-

[1]Defination by National Nanotechnology Initiative (NNI)

platin [$Pt(NH_3)_2Cl_2$ *Cis-Diamminedichloroplatinum or CDDP*] and the controversial reports on the penetration mechanisms, we perform MD simulation in order to provide atomic scale insight. The technique may be applied to many drug molecules but Cisplatin is chosen because it is a powerful anticancer drug with small molecular weight (good for computational efficiency).
The simulation results support the experimental finding that CNT encapsulation facilitates Cisplatin uptake by cancer cells.

1.2 Previous Work

Molecular Dynamics simulations have been applied to study CNT-based drug delivery systems. Hilder and Hill [4] have shown that loading of drug molecules into CNTs and unloading after entering the cell is possible. They performed a series of MD simulations with different drug molecules (Paclitaxel, Doxorubucin) and showed that loading can be achieved by optimizing the CNT size (radius in particular) while unloading (drug release) can be made energetically favourable.

Huajin et. al. [5] showed that a peptide encapsulated inside or attached to the outer surface of CNT can be released via competetive replacement by another peptide or CNT depending on the affintity of the replacing agent to CNT.

Chaban et. al. encapsulated Ciprofloxacin inside a CNT and used near infrared radiation (optical heating) to achieve drug release at 298K. They reported the diffusion coeficient of Ciprofloxacin wich depended on temperature and drug concentration [6]. A comprehensive review of MD simulations of CNTs related to drug delivery is reported in Ref.[7].

The studies of Lopez et. al. showed that CNT cell penetration is a lipid assisted mechanism [8]. Another group used MD simulations to study different CNTs orientations (oblique, parallel and parpendicular) with lipid bilayer and observed that the parpendicular orientation give the smallest membrane poration force [9].

Cipaldi and Vamshi [10] used steered MD (SMD) to study the penetration of DPPC (dipalmitoylphosphatidylcholine) and DPPC/Cholesterol by CNT (no drug). Their studies focused on the force required to puncture the membrane, the CNT internalization process and the effect of cholesterol on the rupture force. They attached the CNT to a dummy atom and the latter was moved at constant velocity. The pulling force, $\mathbf{F}$ needed for the displacement of the dummy atom wan then determined.

Modarrres et. al. also performed SMD to explore the penetration mechanishm of CNT-encapsulated Paclitaxel (PTX) through DPPC [11]. The show that PTX increases the magnitude of the pulling force.

The idea of dragging CNT-encapsulated drug into the lipid bilayer is questionable and not representative of reality (experiment).

Thus, the question remains “what insight can we get from atomistic MD studies of the

transport of CNT-encapsulated drug through a lipid bilayer?" The answer to this question is the aim of this work. Our approach is simple: Find a small, yet potent anticancer drug. Encapsulate this drug in CNT and study the transport of the cargo across a solvated DPPC lipid bilayer under physiological conditions (temperature and pressure). For a very long simulation, we may be able to see exactly how the cargo enters and exits the bilayer. We can also estimate the mobility of the cargo by computing the diffusion coeficient D_A from the Mean Square Dispacement (MSD=$|\mathbf{r}_i(t) - \mathbf{r}_i(0)|^2$) using the celebrated Einstein relation

$$D_A = \lim_{t \longrightarrow \infty} \frac{1}{2td} \langle |\mathbf{r}_i(t) - \mathbf{r}_i(0)|^2 \rangle_{i \in A} \tag{1.1}$$

where $\mathbf{r}_i(t)$ is the position of entity i at time t and 'd' is the dimension of the system.

1.3 Related Experimental Studies

It turns out that there are several experimental work on the cell uptake of Cisplatin (a small drug) encapsulated in CNT. One major work is that of Guven et. al. [12]. They used ultra-short single-walled carbon nanotubes (US-tube) of diameters $\approx 1.4\ nm$ and length $20 - 80nm$ to encapsulate Cisplatin and studied the release of CNT in two different breast cancer cells. They also observe improved cytotoxicity of CDDP@US-tubes over free CDDP.

CHAPTER 2

Molecular Dynamics Simulations

Moelcular Dynamics Simulation is a method for solving for the trajectories $\mathbf{r}(t)$ of atoms as a function of time t. A definition I find all-encompassing is the one given by Ju Li[1]

> "Molecular Dynamics Simulation is a technique by which one generates the trajectories of a system of N particles by numerical integration Newton's equations of motion for a specific interatomic potential, with certain initial conditions (IC) and boundary conditions (BC)."

Consider, for example, a simple atomic system of N particles in a volume V with $i = 1, 2, 3...N$. We can write the equations of motion as

$$\frac{d\mathbf{p}_i}{dt} = \mathbf{F}_i = -\nabla V(\mathbf{r}) \tag{2.1}$$

$$\frac{\mathbf{v}_i}{dt} = \frac{\mathbf{p}_i}{m_i} \tag{2.2}$$

Observe that $\mathbf{r}_i$ represents the complete set of $3N$ coordinates and the net force $\mathbf{F}_i$ acting on atom i is derived from the potential $V(\mathbf{r})$.

The potential energy is a component of the total energy that depends on the positions of atoms. Expressions for the potential energy in terms of the coordinates is known as the functional form of the force field. Each force field uses different functional forms. The equation of the potential energy consist of the bonded (bonds, angles and dihedrals) and

[1] Ju Li *Basic Molecular Dynamics* Department of Materials Science and Engineering, Ohio State University, Columbus, OH, USA

non-bonded (Lennard-Jones and Couloumbic) terms. A general form of the force fieild is given below

$$V = \frac{1}{2}\sum_{bonds} k_r(r-r_0)^2+\frac{1}{2}\sum_{angles} k_\theta(\theta-\theta_0)^2+\frac{1}{2}\sum_{dihedrals} k_\phi[1+\cos(n\phi+\phi_0)]+\frac{1}{2}\sum_{improper} k_\varphi(\varphi-\varphi_0)^2 + \sum_{atom\ i,j>i} 4\epsilon_{ij}\left[\left(\frac{\sigma}{r_{ij}}\right)^{12}-\left(\frac{\sigma}{r_{ij}}\right)^{6}\right]+\sum_{i,\ j>i}\frac{q_iq_j}{4\pi\epsilon_0 r_{ij}} \tag{2.3}$$

In equation 2.3 above, the first four terms are the covalent bond interactions (also called intramolecular interaction) consisting of covalent bond-stretching, angle-bending, proper dihedrals and improper dihedrals, respectively. The variables r, θ, ϕ ,φ are the current bond lengths, bond angles, proper torsions and improper (out of plane distorsions), respectively.

The last two terms are the non-bonded/intermolecular interactions, the Lennard-Jones (12,6) potential and electrostatic couloumbic potential. The Lennard-Jones potential is repulsive at short distances, attractive at long distances and zero at $r = \sigma$. The term $1\backslash r^{12}$ models Pauli's repulsion between atoms when they are brougth very close to each other to an extent that there electronic clouds begin to overlap. The term $1\backslash r^6$ represents the dispersive (or induced-dipole induced-dipole) long-range attractive potential. The parmeters σ and ϵ are usually chosen by fits to experimental data. ˜

2.1 MD Integrators

Solving Newton's equations of motion does not immediately suggest predicting dynammic or static properties. Molcular dynamics algorithms need to be implemented. Once the potential acting on the atom is known, and, hence, the force by differentiation, the position of each atom is updated through an integration algorithm. These integrators will increment the position of an atom from its current position based on the net force, velocity and time step. There are many algorithms for integration of Newton's equations numerically but the most common ones include Varlet algorithm, Leapfrog algorithm and Velocity Verlet algorithm [18].

Verlet Algorithm

The solution of Newton's equations using Verlet algorithm is based on Taylor's series expansion. Expanding the position $\mathbf{r}_A(t)$ of particle A at time $t - \delta t$ and $t + \delta t$ in the Taylor series yield

$$\mathbf{r}_A(t + \delta t) = \mathbf{r}_A(t) + \delta t \frac{d\mathbf{r}_A(t)}{dt} + \frac{(\delta t)^2}{2} \frac{\mathrm{d}^2\mathbf{r}_A(t)}{\mathrm{dt}^2} ... \tag{2.4}$$

$$\mathbf{r}_A(t - \delta t) = \mathbf{r}_A(t) - \delta t \frac{d\mathbf{r}_A(t)}{dt} + \frac{(\delta t)^2}{2} \frac{\mathrm{d}^2\mathbf{r_A(t)}}{\mathrm{dt}^2} ... \tag{2.5}$$

Subtracting equation 2.4 from equation 2.5 gives

$$\mathbf{r}_A(t + \delta t) = 2\mathbf{r}_A(t) - \mathbf{r}_A(t) + (\delta t)^2 \frac{d^2\mathbf{r}_A(t)}{dt^2} + \mathcal{O}(t^4) \tag{2.6}$$

The accelation is obtained from the force $\mathbf{a(t)} = \mathbf{F(t)/m}$. Notice that the velocity does not appear explicitly in the eqution. It is obtained using finite difference formula

$$\mathbf{v}_A(t + \delta t) = \frac{\mathbf{r_A}(\mathbf{t} + \delta \mathbf{t}) - \mathbf{r_A}(\mathbf{t} - \delta \mathbf{t})}{2\delta t} + \mathcal{O}(t^2) \tag{2.7}$$

Eqns. 2.6 and 2.7 comprise the Verlet algorithm. The velocity at time t cannot be calculated untill the position at time $t + \Delta t$ is obtained. This may be a problem if properties of the system, such as kinetic energy, are desired. The Verlet algorithm uses position at time t and $t - \delta t$ and accelation at time t to calculate the new position at time $t + \delta t$. All these have to be stored at every iteration.

Leapfrog Algorithm

Leafrog algorithm is reputed as one of the most stable and accurate technique for use in molecular dynamics [18]. In this scheme, the velocities are first calculated at time $t + \frac{1}{2}\delta t$. These are used to calculate the velocities at time $t + \delta t$ and so on. Consider the Taylor expansion

$$\mathbf{v}_A(t + \frac{1}{2}\delta t) = \mathbf{v}_A(t) + \frac{1}{2}\delta t \frac{d\mathbf{v}_A(t)}{dt} + \frac{(\frac{\delta t}{2})^2}{2!} \frac{\mathrm{d}^2\mathbf{v}_A(t)}{\mathrm{dt}^2} ... \tag{2.8}$$

$$\mathbf{v}_A(t - \frac{1}{2}\delta t) = \mathbf{v}_A(t) - \frac{1}{2}\delta t \frac{d\mathbf{v}_A(t)}{dt} + \frac{(\frac{\delta t}{2})^2}{2!} \frac{\mathrm{d}^2\mathbf{v}_A(t)}{\mathrm{dt}^2} ... \tag{2.9}$$

Subtracting equation 2.9 from 2.8 and rearranging yields

$$\mathbf{v}_A(t + \frac{1}{2}\delta t) = \mathbf{v}_A(t - \frac{1}{2}\delta t) + \delta t \frac{d\mathbf{v}_A(t)}{dt} + \mathcal{O}((\frac{\delta t}{2})^3) \tag{2.10}$$

Or

$$\mathbf{v}_A(t + \frac{1}{2}\delta t) = \mathbf{v}_A(t - \frac{1}{2}\delta t) + \delta t \mathbf{a}_A(t) + \mathcal{O}((\frac{\delta t}{2})^3) \tag{2.11}$$

Using central difference the velocity can be written in the form

$$\mathbf{v}_A(t+\frac{\delta t}{2}) = \frac{\mathbf{r}_A(t+\delta t)-\mathbf{r}_A(t)}{\delta t} + \mathcal{O}(t^3) \tag{2.12}$$

Thus, from equation 2.12, the position is obtained,

$$\mathbf{r}_A(t+\delta t) = \mathbf{r}_A(t) + \mathbf{v}_A(t+\frac{\delta t}{2}) + \mathcal{O}(t^3) \tag{2.13}$$

Equations 2.11 and 2.13 form the so called leapfrog algorithm. A major advantage of this algorithm is the explicit appearance of velocities which is very important when scaling the temperature of the system.

Velocity Verlet Algorithm

Another variant of the Verlet algorithm is the velocity Verlet algorithm. This algorithm only require the storage of positions $\mathbf{r}(t)$, velocities $\mathbf{v}(t)$ and accelations $\mathbf{a}(t)$ of particles that all correspound to the same time step. The position of each particle is obtained from the Taylor series expansion

$$\mathbf{r}_A(t+\delta t) = \mathbf{r}_A(t) + \delta t\frac{d\mathbf{r}_A(t)}{dt} + \frac{(\delta t)^2}{2}\frac{\mathrm{d}^2\mathbf{r}_A(t)}{\mathrm{dt}^2}... \tag{2.14}$$

Setting $t \longrightarrow t+\delta t$ in equation 2.5 gives

$$\mathbf{r}_A(t+\delta t-\delta t) = \mathbf{r}_A(t) = \mathbf{r}_A(t+\delta) - \delta t\frac{d\mathbf{r}_A(t+\delta)}{dt} + \frac{(\delta t)^2}{2}\frac{\mathrm{d}^2\mathbf{r}_A(t+\delta)}{\mathrm{dt}^2}... \tag{2.15}$$

Substituting equation 2.15 into equation 2.14 and rearranging gives the velocity

$$\mathbf{v}_A(t+\delta t) = \frac{d\mathbf{r}_A(t)}{dt} + \frac{\delta t}{2}\Big(\frac{d^2\mathbf{r}_A(t)}{dt^2} + \frac{d^2\mathbf{r}_A(t+\delta t)}{dt^2}\Big) \tag{2.16}$$

2.2 Boundary Conditions

MD simulations are performed on a few number of particles in a simulation cell. Periodic Boundary Conditions (PBCs) enable macroscopic properties to be calculated from these few particles by replicating the primary cell in all simulated directions as image cells so as to form an infinite system. There are no walls on the surface of the primary cell. Particles can move through the boundaries. This completely eliminate surface effects associated with systems of molecules with small sizes. Image cells are exact copies of primary cells i.e., they have the same shape, size, number of particles (with the same positions and momenta).

2.3 Thermostats and Barostats

Ideally, MD simulation samples the microcanonical ensemble because Newtonian mechanics implies that the energy (and the momentum) are conserved quantities of motion [15]. The microcanonical ensemble NVE (conatant number of particls N, constant volume V, constant energy E) does not directly correspond to experimental conditions. Most experimental conditions correspound to either canonical ensemble (NVT-conatant number of particles N, constant volume V, constant temperature T) or isobaric-isothermal (NPT-conatant number of particles N, constant volume P, constant temperature T) and therefore it is often necessary to control temperature and/or pressure. This is done using using a thermostat and/or barostat, respectively.

Thermostats commonly used in MD simulations include direct velocity-recaling method, Berendsen Thermostat [31], Anderson Thermostat [32] and Nosé-Hoover Thermostat [36]. What is provided here is far from exhaustive as this would mean writing a textbook on MD simulation instead of applying its principles to study transport of encapsulated drugs. However, details of what follows could be found in Ref [16] and Ref [17].

Velocity Rescaling

Velocity-rescaling is a constraint method where the velocities of particles are rescaled with a scaling factor λ in order to fix the temperature during simulation. Initial velocities are described by the *Maxwell-Boltzmann's distribution*

$$P(v_{i,\alpha}(0)) = \sqrt{\frac{m_i}{2\pi k_B T}}\ \exp^{-\frac{m_i v_{i,\alpha}^2(0)}{2k_B T}} \tag{2.17}$$

Temperature adjustment can be achieved by scaling all velocities at each time step (or after a preset number of steps) according to

$$\mathbf{v}_i \longrightarrow \lambda \mathbf{v}_i \tag{2.18}$$

$$\lambda = \sqrt{\frac{T_0}{T(t)}} \tag{2.19}$$

Where T_0 is the desired temperature and $T(t)$ is the actual kinetic temperature. $T(t)$ is obtained from the average kinetic energy of the system via the equipartion theorem

$$\frac{1}{2} N_{df} k_\beta T = \langle K.E \rangle = \sum_i^N \langle \frac{1}{2} m_i v_{i,\alpha}^2 \rangle \tag{2.20}$$

$$\implies T = \frac{1}{N_{df} K_\beta} \sum_i^N \langle m_i v_{i,\alpha}^2 \rangle, \tag{2.21}$$

where, m_i is the mass of the particle i, $v_{i,\alpha}$ is the $\alpha-$th component of its velocity ($\alpha = x, y, z$), N_{df} is the total number of degrees of freedom[1] of the system.
This method is straightforward to implement and good for initiation phase (warm up).

Berendsen Thermostat

To alleviate the problem of velocity rescaling, Berendsen introduces weak coupling to an external heat bath that suppresses fluctuations in temperature. Thus, instead of scaling the velocities to give the exact temperature, you scale the velocities in the direction of the desired temperature. This is achieved by adding a frictional term to the equation of motion:

$$m_i \frac{d\mathbf{v}_i}{dt} = \mathbf{F}_i - m_i\gamma(\frac{T_0}{T} - 1)\mathbf{v}_i \tag{2.22}$$

so that the rate of change of temperature is proportional to the difference in temperatures

$$\frac{dT}{dt} = \frac{1}{\tau}(T - T_0), \tag{2.23}$$

where, τ, the *coupling constant* or *time scale of heat transfer* determines how tight the bath and the system are coupled. The frictional constant, γ, is related to the coupling constant by $\tau = (2\gamma)^{-1}$ Observe that integrating equation 2.23 the system temperature decays exponentially to the desired value

$$T = T_0 + Cexp\Big(-\frac{t}{\tau}\Big) \tag{2.24}$$

with a scaling factor given by

$$\chi = \Big[1 + \frac{\Delta t}{\tau}\Big(\frac{T_0}{T} - 1\Big)\Big]^{1/2} \tag{2.25}$$

The Berendsen scheme is very efficient in reaching the desired temperature as such it can be used for equilibration run in MD. Unfortunately it does not generate the correct canonical ensemble for small systems, althought correct results of some properties were reported for large systems [20]

Anderson Thermostat

Anderson proposed that the system is thermally coupled to a fictitious heat bath at a desired temperature. The coupling to a heat bath is achieved by stochastic collision that

[1] $N_{df} = 3N - N_c$, where N is the number of atoms and N_c is the number of constraints.

acts once in a while on randomly selected particles. Particle(s)[2] are randomly chosen and the frequency of stochastic collisions is governed by Poisson distribution

$$P(t;\nu) = \nu e^{-\nu t} \tag{2.26}$$

where ν is the stochastic collision frequency which determine the strength of the coupling to heat bath and t is the time of collision. In the limit of an infinitely long trajectory averaged over many collisions, the Anderson thermostat can be used to generate the correct canonical ensemble. i.e the trajectory generated can be used to calculate time averages of any quantity according to

$$A = \lim_{t\to\infty} \int_0^t A(q^N(t'), P^N(t'))dt' \tag{2.27}$$

However, the presence of random collision causes the velocities to decorrelate (lose memory of previous values). Thus, the method should not be used to measure dynamical properties such as the diffusion coeficient.

Nosé-Hoover Thermostat

Originally proposed by Shuichi Nosé [35] and subsequently improved by William G. Hoover [36], the Nosé-Hoover thermostat introduces an extended system method for controlling the temperature by coupling to a heat bath with an artificial variable s of mass $Q > 0$. The value of Q determines the strength of the coupling between the reserviour and the real system. Thus, the original Lagrangian is now extended to contain additional artificial coordinates s and its velocity $\dot{s}$. The real variables $(\mathbf{q}_i' \ , \dot{\mathbf{q}}_i')$ are related to the artificial variables as follows:

$$\mathbf{q}'_i = \mathbf{q}_i \qquad \dot{\mathbf{q}}'_i = \frac{\dot{\mathbf{q}}_i}{s} \qquad t = \int_0^t \frac{dt}{s} \tag{2.28}$$

Observe that the transformation above is equivalent to scaling by

$$dt' = \frac{dt}{s}$$

The extended Lagrangian is

$$L_{ext} = T - V + T_s - V_s$$

$$L_{ext} = \frac{1}{2}\sum_i m_i s^2 \dot{q}_i^2 \ - \ V(q) \ + \ \frac{1}{2}Q\dot{s}^2 \ - \ gk_B T ln \ s \tag{2.29}$$

T and $V(q)$ are the are the usual kinetic and potential energy of the original system, respectively. The last two terms in Eq. 2.29 are the kinetic T_s and potential V_s energy,

[2] *Single particle approach* is when the velocity of one particle is altered by stochastic collision. *Massive collision approach* is when velocities of all particles are reselected at once. Details in ref[15]

respectively, associated with the virtual particle(s). The parameter, g is the number of degrees of freedom and T is the specified temperature. The momenta conjugate to q_i and s_i are

$$P_i = \frac{\partial L_{ext}}{\partial \dot{q}_i} = m_i s^2 \dot{\mathbf{q}}_i \qquad P_s = \frac{\partial L_{ext}}{\partial \dot{s}} = Q\dot{s}^2$$

Using the Euler-Lagrange Equation, the Nosé equations of motion are

$$\ddot{q} = \frac{F}{ms^2} - \frac{2\dot{q}\dot{s}}{s} \tag{2.30}$$

$$\ddot{s} = \frac{1}{Qs}\Big(\sum_i ms^2\dot{q}_i^2 - gk_BT\Big) \tag{2.31}$$

The Nosé-Hoover method can be shown to generate the correct canonical ensemble. Large values of Q (i.e $Q \longrightarrow \infty$) represent loose coupling (or poor temperature control) which generates the microcanonical ensemble. On the other hand, small Q (i.e Q$\longrightarrow$ 0) implies tight coupling which leads to high frequency oscillations.

2.4 GROMACS

GROMACS: GROningen MAchine for Chemical Simulations.

GROMACS is a molecular dynamics suite of computer programs designed for the simulation of biochemical molecules (proteins, lipids, etc.).

It is a free software available under the General Public License. It was originally developed at the department of biophysical chemistry, University of Groningen, Netherland between 1991 and 2001. Since 2001, GROMACS is maintained by a team at the Royal Institute of Technology and Uppsala University, Sweden. It has a large selection of built-in tools for trajectory and energy analysis, automated topology builder for many biomolecules, support for different force fieilds, ability to run in parallel, and many more. Fig. 2.4 shows a typical GROMACS flowchart for MD simulations.

MD simulation usually starts with a coordinate/structure file from a Protein Data Bank or any other biomolecular repository. The coordinate file is then used to generate gromacs compatible file (input.gro), topology file (topol.top) and position restrain file (posre.itp), using a gromacs utility called **pdb2gmx**. As can be seen from the flowchart, output files generated in one step are used as input files in the subsequent steps. This continues untill trajectory (traj.trr) and energy (ener.edr) files are finally produced. The final output files (i.e. energy and trajectory files) are then analysed to extract information about properties of interest.

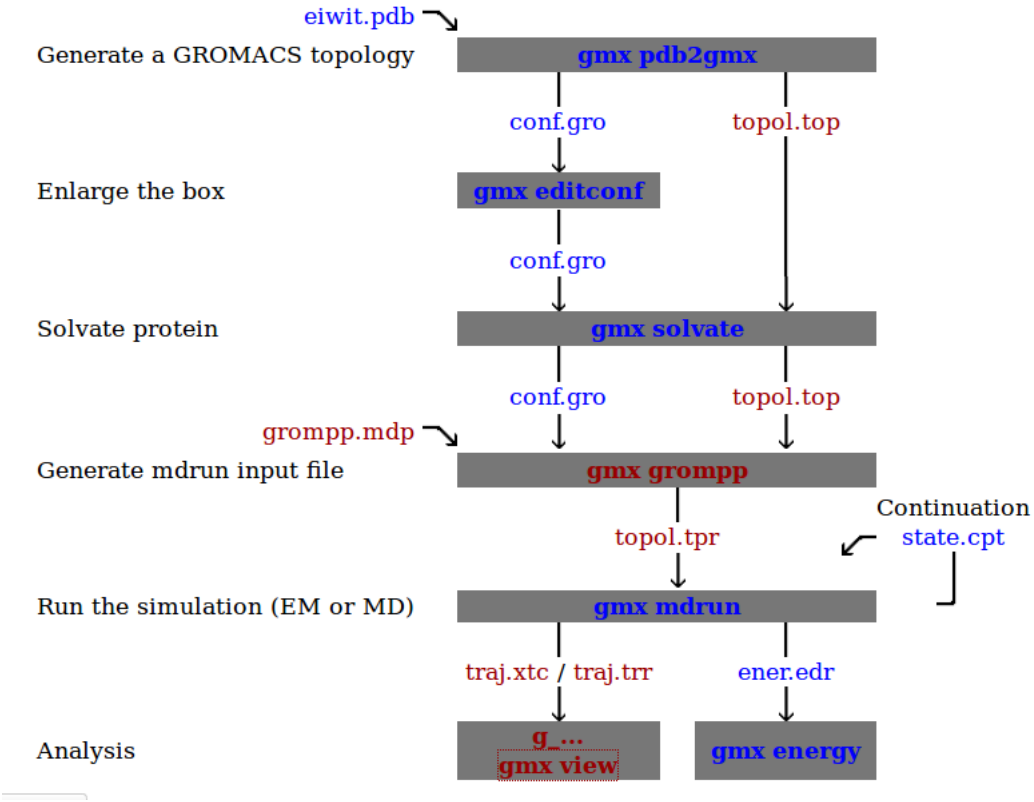

Figure 2.1: GROMACS Flowchart for MD simulation. Figure taken from http://manual.gromacs.org/online/flow.html

CHAPTER 3

Computational Details

3.1 General Approach

GROMACS 5.0.2 program [21] was used to perform all simulations, and VMD 1.9.1 was used for visualization [22]. Water molecules were modelled by the simple point charge (SPC) of Ref. [23]. The simulation system consisted of 64 DPPC (dipalmitoylphosphatidylcholine) molecules previously equilibrated at 323K, a (11,11) armchair SWCNT, a Cisplatin molecule and water molecules to solvate the system.

A (11,11) armchair single-wall CNT with a length of 2.0 nm and diameter of 1.492 nm was constructed using VMD nanotube builder and VMD was also used for the encapsulation of Cisplatin. CNT was electrostatically neutral while partial charges were assigned to other atoms. Parameters for interaction involving carbon atoms of CNT were taken from optional potential for liquid simulation (OPLS) force field [24].

Cisplatin toplogy file was generated and included in a master topology file [1]. Charges in cisplatin molecule are as listed in Table 3.3. They were determined by electrostatic potential fits to ab initio density functional theory (DFT) calculations. The structure of Cisplatin is given in Fig. **??** (a).

The DPPC lipid bilayer was obtained from Tielman's website [26] and correspound to fully hydrdrated lipid molecules ($\approx$ 30 waters per lipid) previously equilibrated at a

[1] This eliminated the need for pdb2gmx since we are not using any of the built-in force fields in the GROMACS computer package

temperature of $323K$ and at pressure 1 *bar* [27]. The toplogy file from the Tieleman group also included a force field used for the lipids, the widely used Berger lipids, which is a hybrid between GROMOS98 and OPLS force fields [33]

Unless mentioned otherwise all simulations were carried out with a timestep of 1 fs ($2.0 \times 10^{-15} seconds$) and periodic boundary conditions were applied in all three directions.

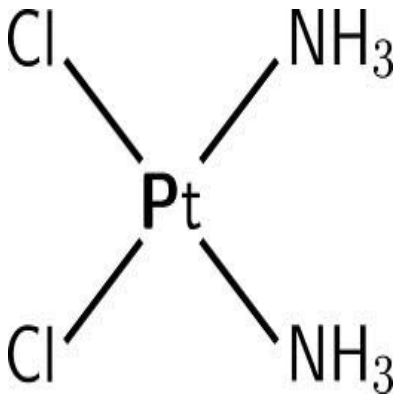

Figure 3.1: Cisplatin molecule

3.2 System I

This system consists of 64 DPPC molecules, 4652 water molecules and a Cisplatin molecule, Fig.3.2.

A triclinic simulation box was constructed with the dimension 47.245 X 42.312 X 99.505$\mathring{A}^3$. Cisplatin was initially placed close to the lipid molecules in the absence of water. The steepest decent algorithm was used to minimize the Cisplatin-DPPC system. Then this system was solvated with 4652 water molecules and the potential energy was minimized again.

Following the minimization, $constant - NPT$ simulation for 10 ns was made. The first 200 ps of the simulation was considered the equilibration phase and therefore all properties of interest were measured after the first 200 ps. The system was thermostated using a using a Nosé-Hoover thermostat with a coupling time of 0.5ps. The Martyna-Tuckerman-Tobias-Klein (MTTK) [34] barostat was used with an applied pressure of 1 bar. Long range electrostatic interaction was calculated using the Particle Mesh Ewald method. The van der Waals interaction and the short-range coulomb interaction cutoff were kept at 1.2 nm. The GROMACS parameter file for this run is given in APPENDIX C

3.3 System II

This system consist of everything in system I but Cisplatin is encapsulated inside a CNT, see Fig. 3.3. We used the experimental insight that the perpendicular orientation of CNT gives the smallest poration force compared to oblique or parallel orientation of CNT to the lipid bilayer [25].

Table 3.1: Simulated Systems Consisting of DPPC, a Carbon Nanotube (CNT), Cisplatin (CDDP) and water molecules (SOL).

System	DPPC molecules	CDDP	$H_2O(SPC\ molecules)$	CNT	Total number of atoms
I	64	1	4652	0	17161
II	64	1	4553	1	17084

Table 3.2: Charges of the atoms in Cisplatin molecule obtained from ab initio calculations.

S/N	Mass	Atom	Charge, q
1	195.078	Pt	-0.125704
2	35.453	Cl	-0.289005
3	35.453	Cl	-0.289005
4	14.067	N	+0.351856
5	14.067	N	+0.351856

Charge on Nitrogen atoms is average charge i.e

$$q_N = \overline{q}_N + \overline{q}_H$$

where $\overline{q}_H$ is the average charge on 6 hydrogen atoms of Cisplatin molecule.

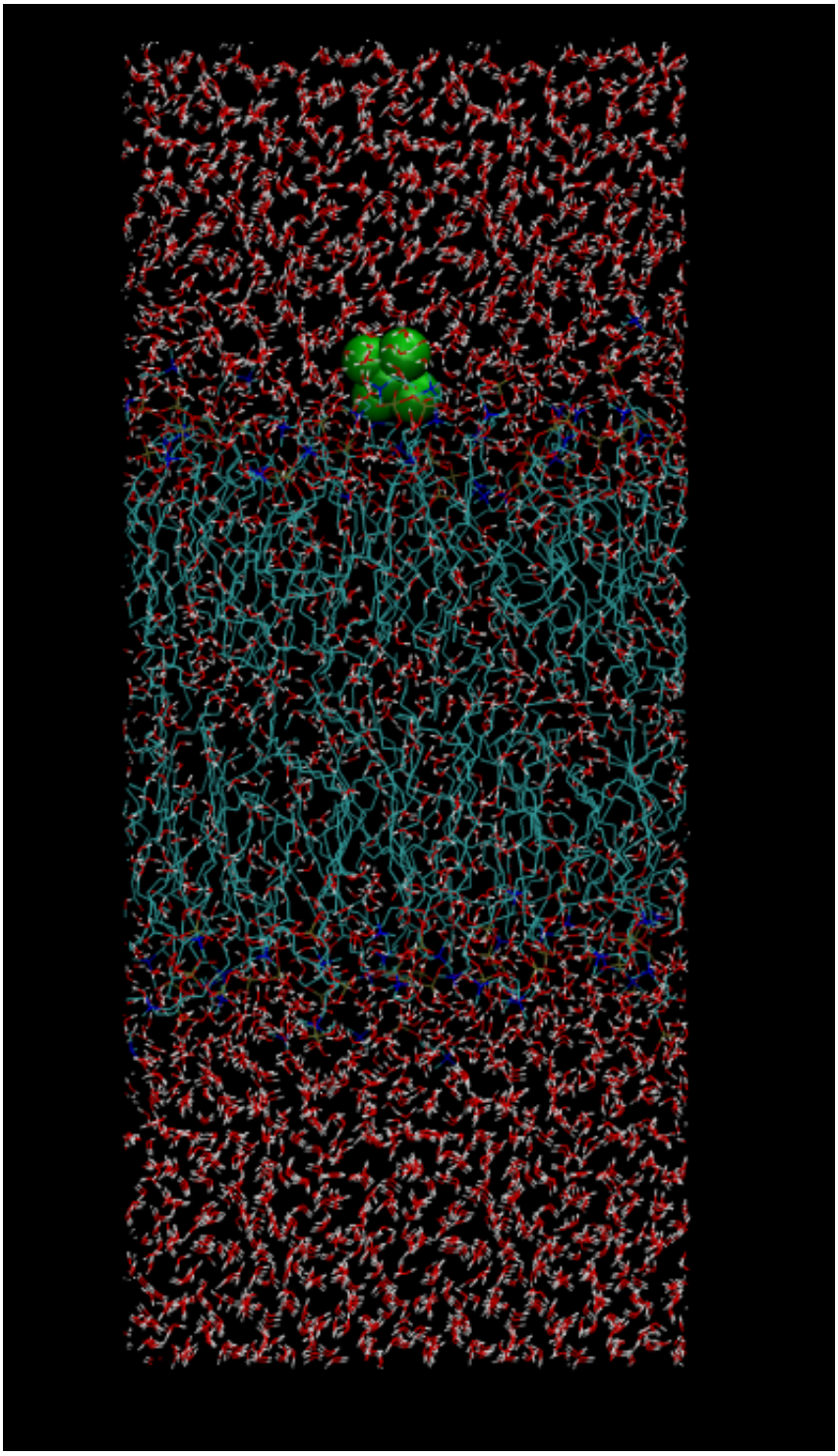

Figure 3.2: SYSTEM I initial configuratione

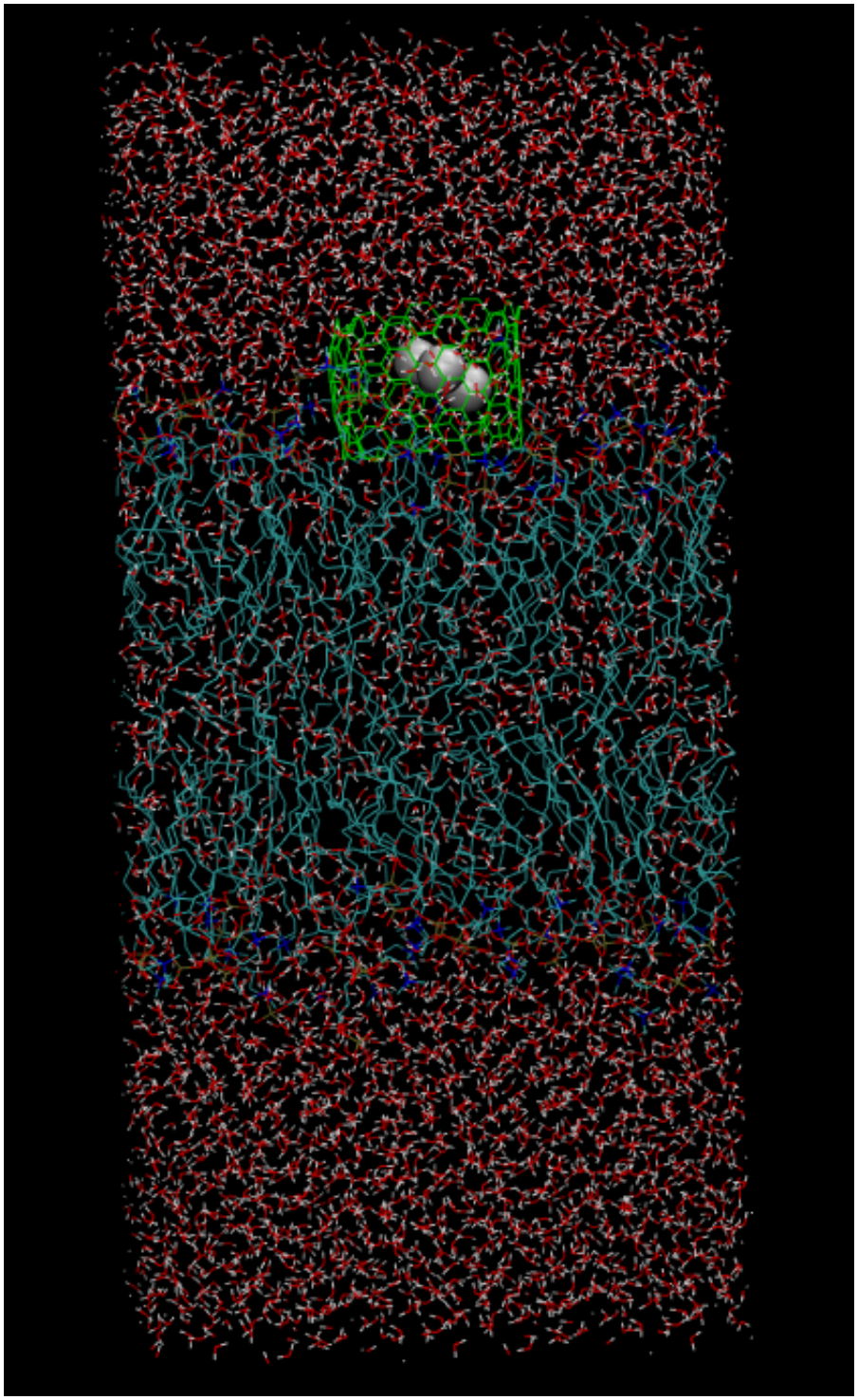

Figure 3.3: SYSTEM II initial configuration, see Table 3.3 for details

CHAPTER 4

Results and Discussion

4.1 Minimization

Energy minimization aims to relax the system to the configuration of lowest potential energy. In the process, any local strain or bad contacts are removed. Fig.4.1 and Fig. 4.1b shows the potential energy plot for systems I and II, respectively.

For system I, the potential energy decreases steadily to its lowest value $-2.75\times10^5 kJ/mol$ while the maximum force is on Pt atom $F_{max} = 8.31 \times 10^3 kJmol^{-1}m^{-1}$. For system II, the minimum potential energy obtained was $= -2. \times 10^4 (kJ/mol)$ and $F_{max} = 7.04 \times 10^4 kJmol^{-1}m^{-1}$. See APPENDIX D for GROMACS parameter file (em.mdp) used in controlling the minimization.

4.2 Equilibration

The aim of equilibration is to ensure that the system attains the right ensemble. As explained in the previous chapter, the first 200 ps of the production run was considered as equilibration.

Fig.4.2a shows that the temperature of the system quickly reaches the target value (310 K), and remains stable over the rest of the equilibration. This is expected because DPPC was previously equilibrated close to the temperature. Observe that in Fig.4.2b, the presssure fluctuates widely approximately about the preset value (1 bar). The potential energy plot shows an initial increase with time and then stabilizes, Fig.4.2. The Kinetic and Total Energy of the system also stabilized, as shown in Fig.4.2a and Fig.4.2b, respectively.

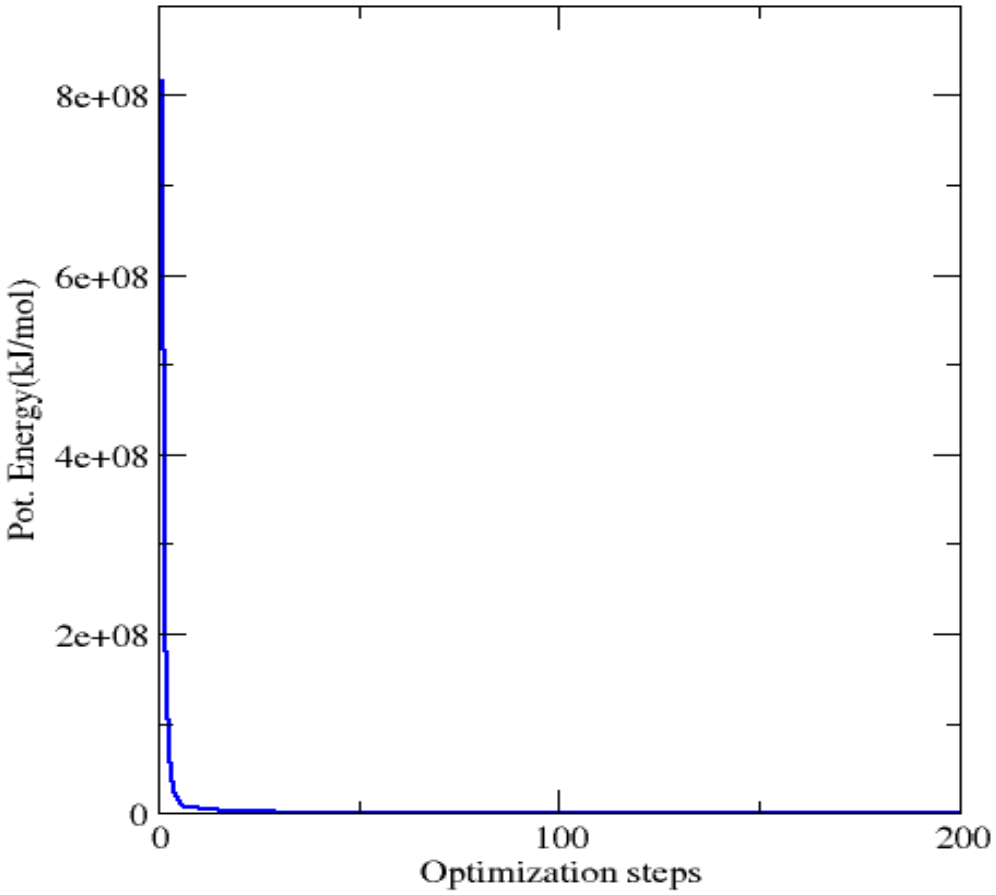

a)

Figure 4.1: Potential Energy for CDDP in solvated DPPC showing steady convergence to a minimum

4.3 Production Run

Minimization and and equilibration were short runs used to get the system into the right ensemble-NPT in our case. We are interested in the dynamical properties of the system. However, it is worth observing some structural changes in the system over the couse of the simulation.

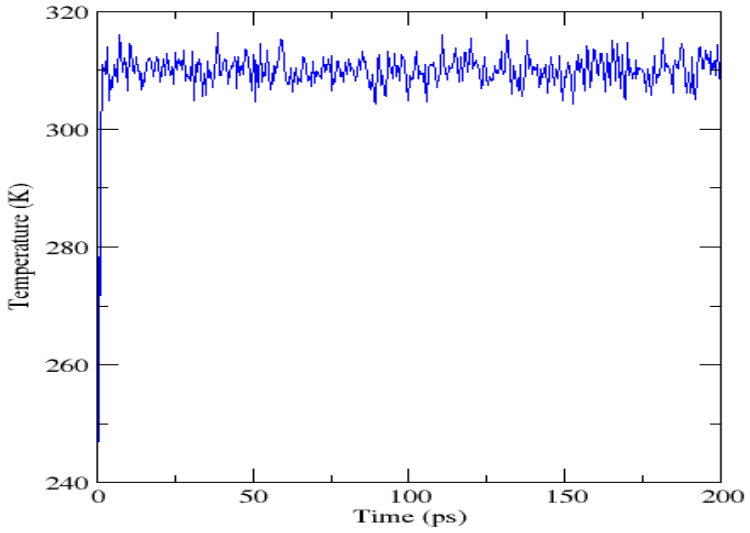

a)

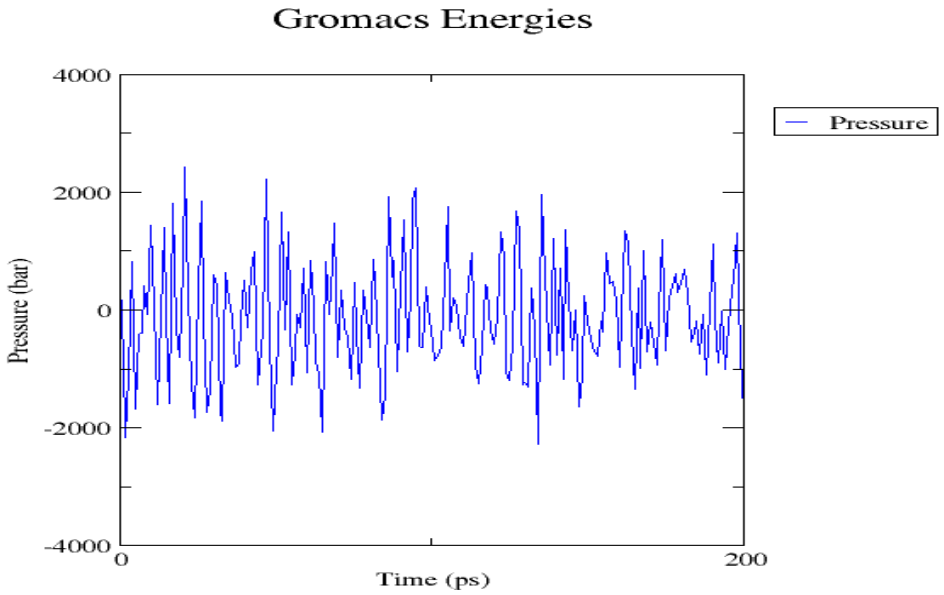

b)

Figure 4.2: (a) Temperature and (b) Pressure for for system I

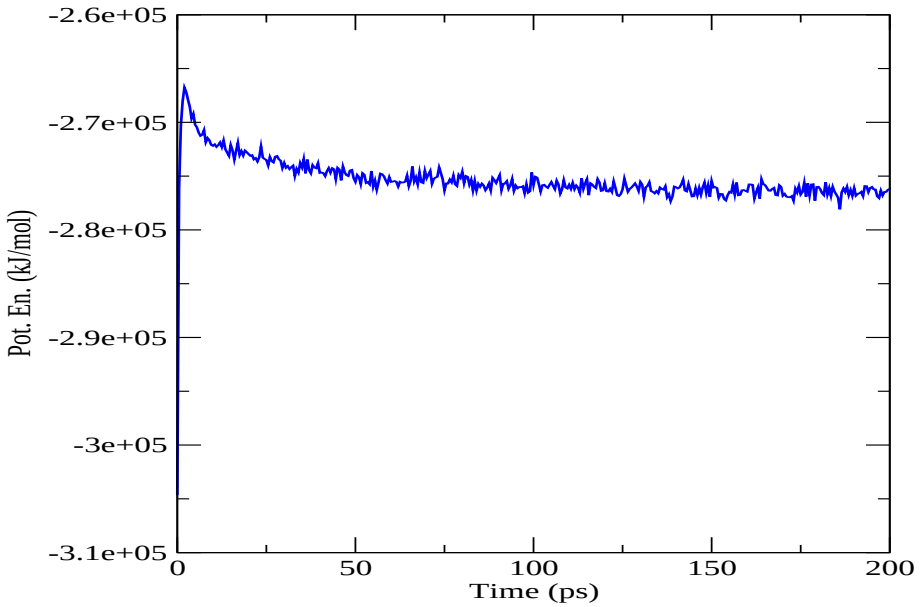

Figure 4.3: Potential energy for 200ps equilibration

4.3.1 Root Mean Square Deviation (RMSD)

RMSD is the spatial difference between two structures. It shows how different the simulated structure is from a reference structure.

$$RMSD = \sqrt{\frac{1}{N}\sum_{i}^{N}(\mathbf{r}_i(t) - \mathbf{r}_i^{ref}(0))^2}$$

The RMSD plot, Fig.4.3.1, shows that the structure is stable but it differs from the structure at time $t = 0$ due energy minimization and equilibration.

4.3.2 Diffusion Coefficient

Molecular dynamics trajectories were used to calculate the diffusion coefficient of free Cisplatin and CNT-encapsulated Cisplatin in systems I and II, respectively. In each case, D_A is calculated from the Mean Square Dispacement (MSD) in one direction. In GROMACS,

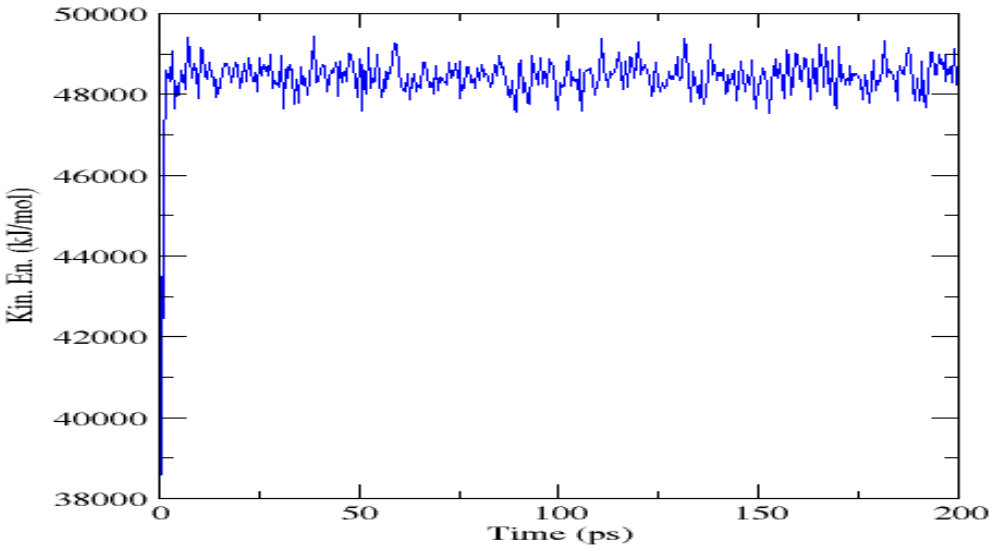

(b)

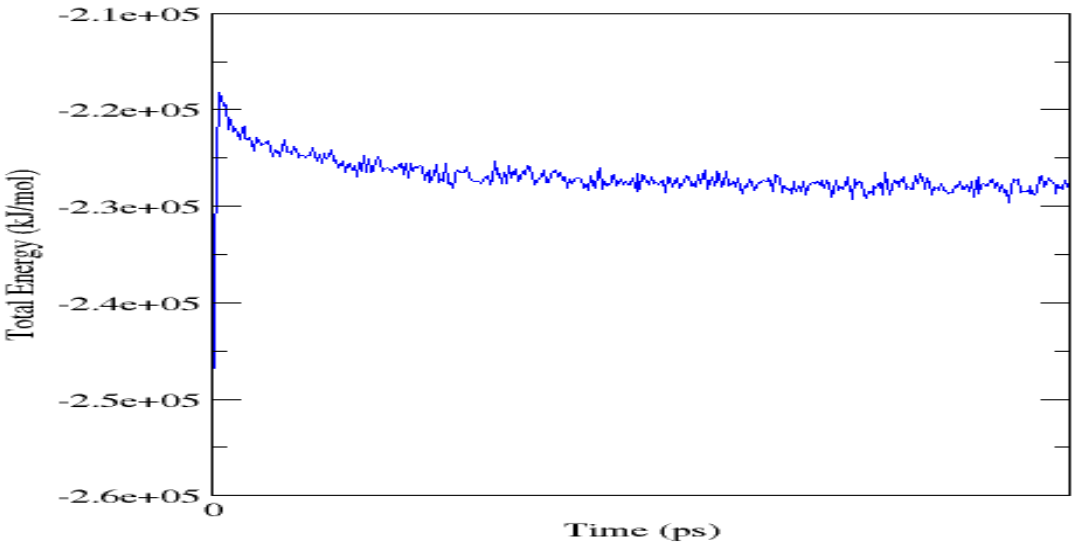

(b)

Figure 4.4: (a) Kinetic and (b) Total energy for system I after 200ps equilibration

atoms can be grouped based on their residue type. Thus, using GROMACS utility called **gmx msd**[1], the diffusion coeficients were obtained as follows

$$D_{CDDP} = \lim_{t \longrightarrow \infty} \frac{1}{2td} \langle |\mathbf{z}_i(t) - \mathbf{z}_i(0)|^2 \rangle_{i \in A} i \in A^2 \tag{4.1}$$

$$D_{CNT+CDDP} = \lim_{t \longrightarrow \infty} \frac{1}{2td} \langle |\mathbf{z}_i(t) - \mathbf{z}_i(0)|^2 \rangle_{i \in A}{}^3 \tag{4.2}$$

Where $d = 1$ since we are interested only in motion along z direction (perpendicular to the lipid bilayer). The results are given in Table 4.3.2 and the graphs are shown in Figure .4.3.2

Table 4.1: Diffusion Coefficient for free CDDP and CNT-encapsulated CDDP.

System	$D_s(10^{-5}\ cm^2 s^{-1})$	Error Estimate
CDDP	0.2196	0.2591
CNT-CDDP	0.6149	0.1336

4.3.3 Structural Changes

To illustrate the effect of CNT encapsulation on the transport of Cisplatin across the lipid bilayer, we took snapshots at different time steps of the simulation. In System I, Fig.4.3.3, it can be seen that the polar drug, Cisplatin, did not enter the lipid bilayer throughout the simulation time of 10ns. It avoids the hydrophobic lipid environment and moves towards water-rich region in the simulation box.

In System II, Fig.4.3.3, the CNT (containing the Cisplatin molecule), was placed very close to the surface of the lipid bilayer. Cisplatin molecule was encapsulated inside the CNT. The penetration was slow during the first 4 ns but increased as soon as the CNT contacted the hydrophobic tail of the lipid. This increase could be as a result of a *hydrophobic pull* on CNT by the lipid tail. At the end of the 10 ns run, more than 50% of the CNT was engulfed by the membrane. Thus, given a longer simulation, 100-200ns, we may be able to see exactly how the CNT-encapulated Cisplatin system enters and exits the lipid bilayer.

[1] A special index group for CNT and CDDP atoms was made using GROMACS utility called $gmx\ make - ndx$.

[2] For all CDDP atoms

[3] For all CNT and CDDP atoms

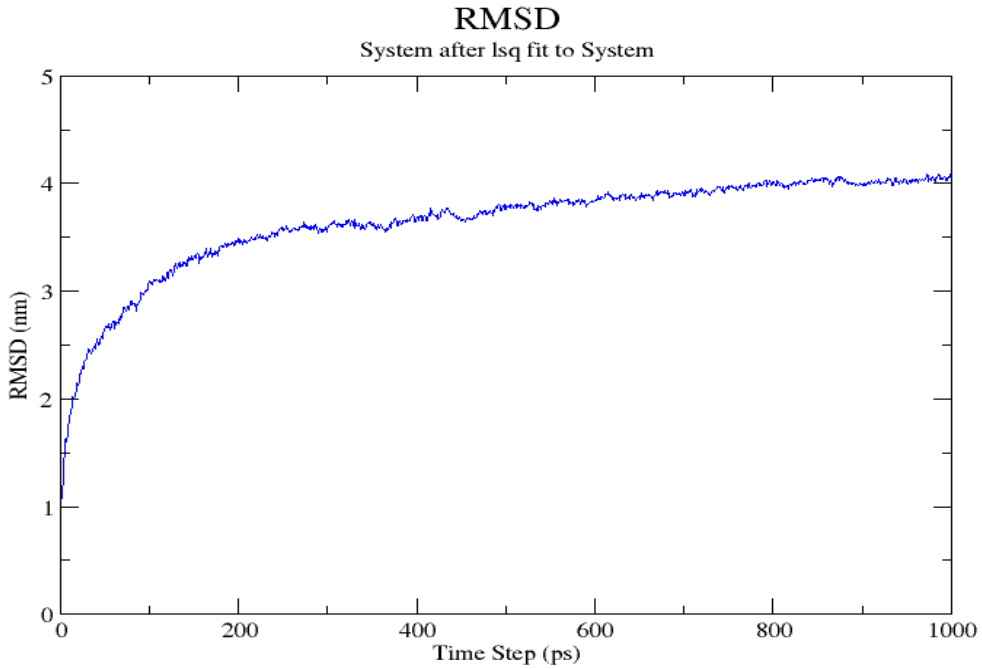

(a)

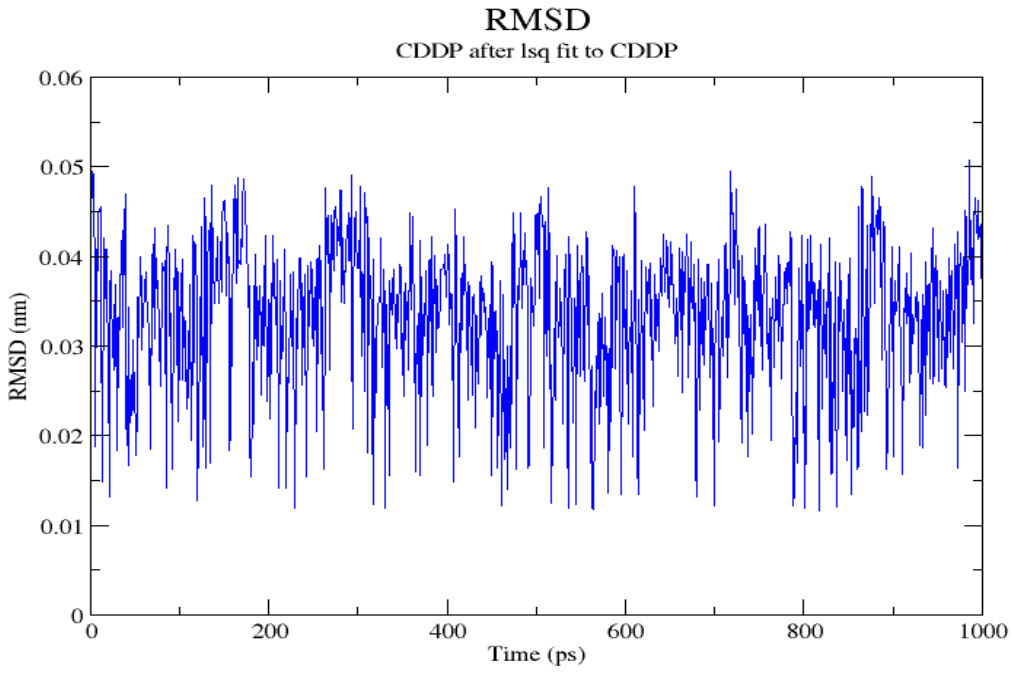

(b)

Figure 4.5: RMSD for (a) system I (b) Cisplatin

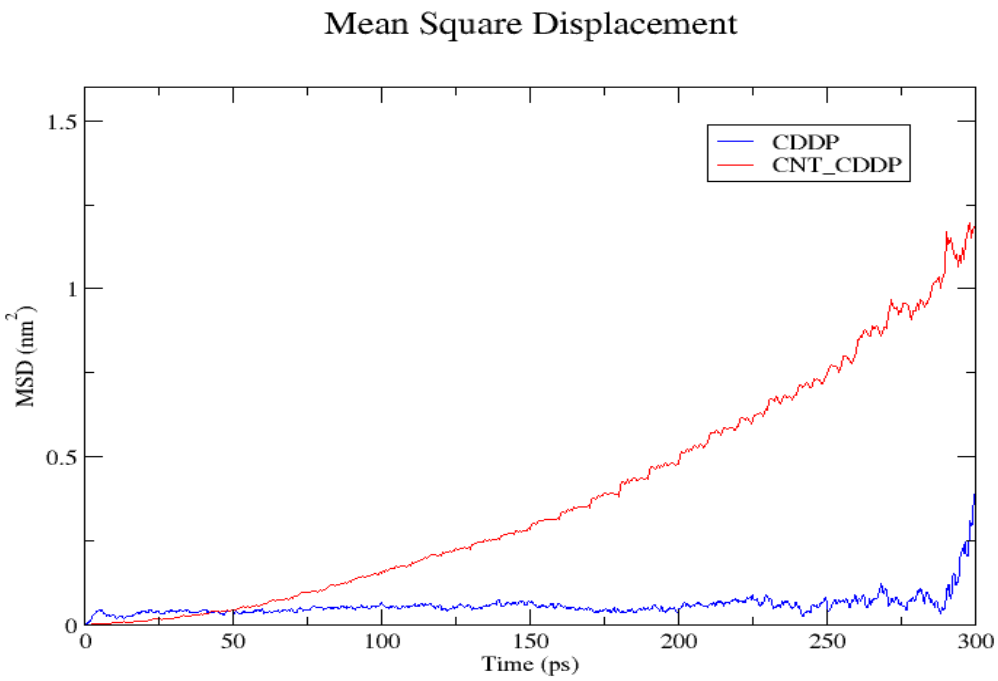

Figure 4.6: MSD for Cisplatin in System I (CDDP, blue line) and CNT+Cisplatin (CNT-CDDP) in System II

(a)

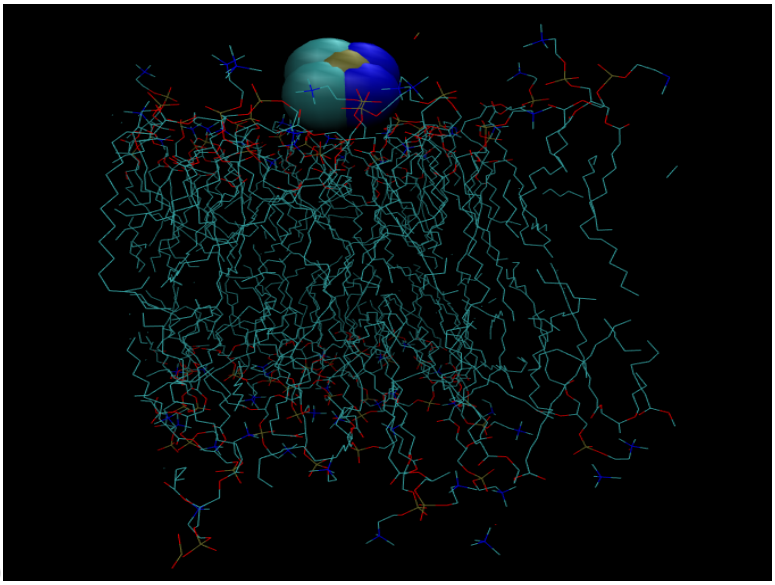

(b)

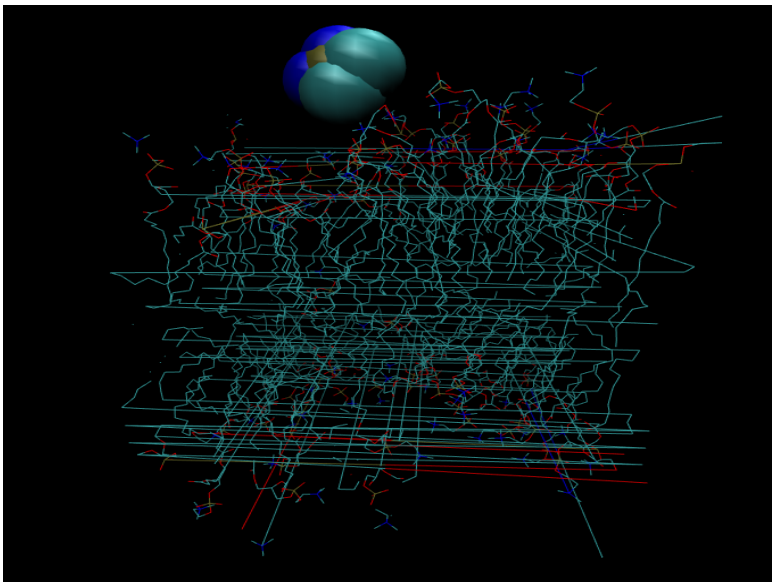

(b)

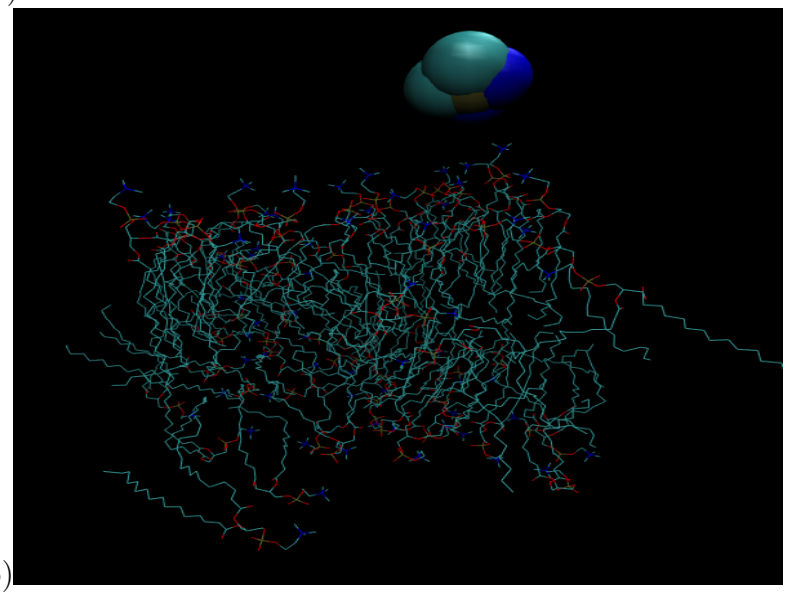

Figure 4.7: Snapshots of Cisplatin with DPPC lipid bilayer at different simulation time steps (a) Initial configuration, (b)1ns later, when the hydrophylic drug starts to move towards water molecules. Water molecules are removed for clarity.

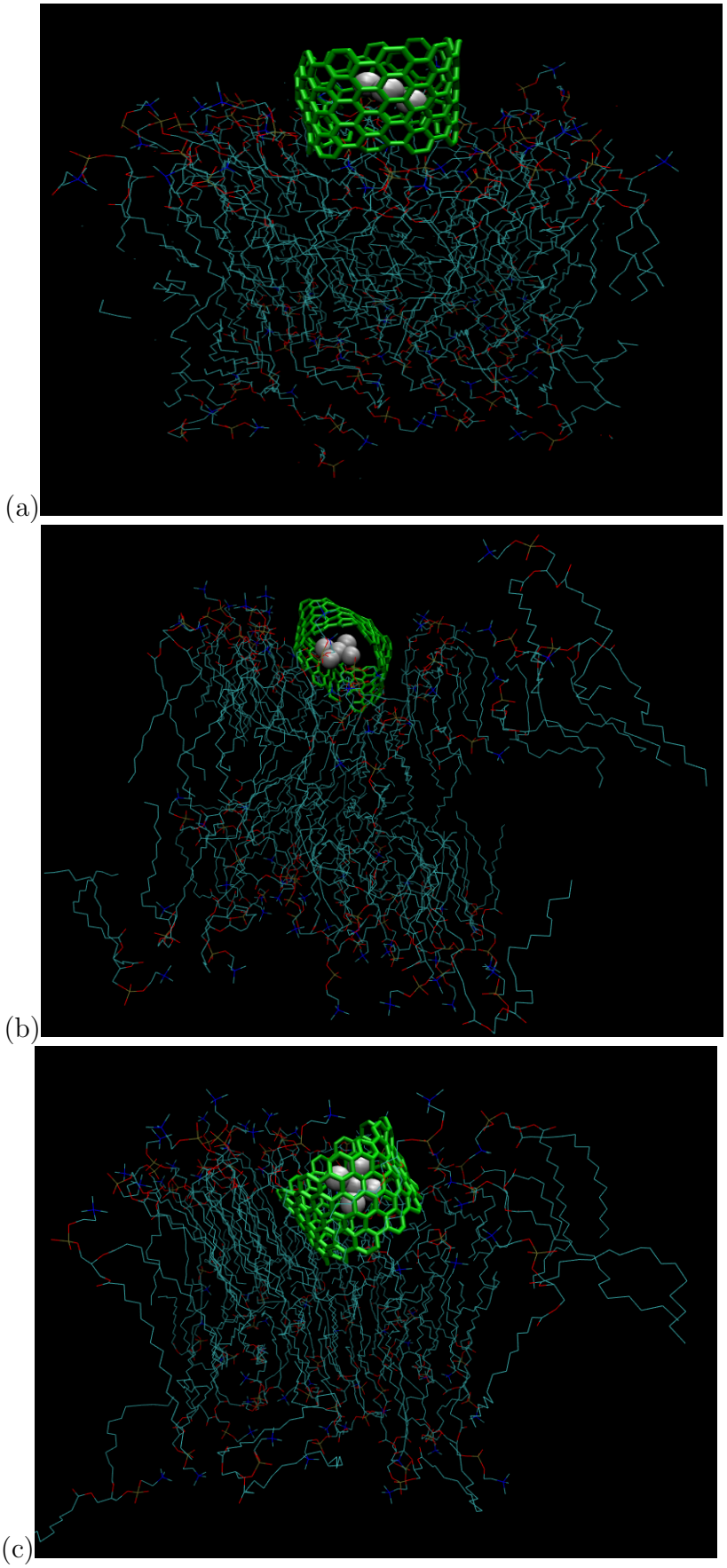

Figure 4.8: Snapshots of CNT-encapsulated Cisplatin penetration through lipid bilayer at different simulation times (a) Initial configuration, (b) 1ns later when the cargo starts to penetrate, (c)10ns later, the cargo is engulfed in the lipid bilayer. For clarity, Water are removed from the picture.

CHAPTER 5

Conclusion and Future Work

We used Molecular Dynamic simulations to study the transport of CNT-encapsulated Cisplatin through a DPPC bilayer. While free Cisplatin was not able to penetrate the lipid bilayer and actually moved away from the lipid, CNT-encapsulated Cisplatin penetrated the bilayer. Thus, CNT-encapsulation facilitated the transport of the polar anticancer drug across DPPC, as observed experimentally in cancer cells.

The simulations were run in the NPT ensemble under physiological conditions (310K and 1 atm) and the size (1.492nm diameter) of the nanotube is comparable to that used in experiments (1.40nm diameter, Guven et. al. [12]). The choice of the ensemble and the size of CNT was such that our results could serve as a computational microscope to experimentalist.

We have restrained ourselves in this work to transport of CNT-encapsulated drug across lipid bilayer. Future work may include the effect of temperature, CNT size (length and diameter) on the CNT+CDDP penetration process and on how different drugs interact with CNT. Finally, the approach used in this work may be applied to many drug molecules.

APPENDIX A

GROMACS parameter file for Energy Minimization

; em.mdp - used as input into grompp (a pre-processor) to generate em.tpr (a binary file)
;which is then used for energy optimization
; Parameters describing what to do, when to stop and what to save
integrator = steep ; md Algorithm
emtol = 10.0 ; Stop minimization when the maximum force $<$ 1000.0 $kJ/mol/nm$
emstep = 0.01 ; Energy step size
nsteps = 50000 ; Maximum number of (minimization) steps to perform
cutoff-scheme = Verlet
verlet-buffer-tolerance = 0.005

; Parameters describing how to find the neighbors of each atom and how to
;calculate the interactions
nstlist = 20 ; Frequency to update the neighbor list and long range forces
ns-type = grid ; Method to determine neighbor list (simple, grid)
rlist = 1.0 ; Cut-off for making neighbor list (short range forces)
coulombtype = PME ; Treatment of long range electrostatic interactions
rcoulomb = 1.2 ; Short-range electrostatic cut-off
rvdw = 1.2 ; Short-range Van der Waals cut-off
pbc = xyz ; Periodic Boundary Conditions in all directions

APPENDIX B

GROMACS parameter file for NPT ensemble simulation

```
title = NPT run
;define = -DDEBUG -DPOSRES ; position restrain the protein
; Run parameters
integrator = md-vv ; Velocity-verlet integrator
nsteps = 10000000 ; 1fs * 10000000 = 10ns
dt = 0.0010 ; 2 fs
; Output control
nstxout = 500 ; save coordinates every 0.5 ps
nstvout = 500 ; save velocities every 0.5 ps
nstenergy = 500 ; save energies every 0.5 ps
nstlog = 500 ; update log file every 0.5 ps
; Bond parameters
continuation = no ; Restarting after optimization
constraint-algorithm = lincs ; holonomic constraints
lincs-iter = 2 ; accuracy of LINCS
lincs-order = 4 ; also related to accuracy
; Neighborsearching
cutoff-scheme = Verlet
verlet-buffer-tolerance = 2.6e-03
ns-type = grid ; search neighboring grid cells
nstlist = 20 ; 20 fs, largely irrelevant with Verlet scheme
rlist = 1.0
rcoulomb = 0.7 ; short-range electrostatic cutoff (in nm)
rvdw = 0.7 ; short-range van der Waals cutoff (in nm)
; Electrostatics
coulombtype = PME ; Particle Mesh Ewald for long-range electrostatics
pme-order = 4 ; cubic interpolation
fourierspacing = 0.16 ; grid spacing for FFT
; Temperature coupling is on
tcoupl = Nose-hoover ; Thermostat
tc-grps = DPPC CNT CDDP SOL ; four coupling groups - more accurate
tau-t = 0.5 0.5 0.5 0.5 ; time constant, in ps
ref-t = 310. 310. 310.0 310.0 ; reference temperature, one for each group, in K
; Pressure coupling is on
```

pcoupl = MTTK ; Martyna-Tuckerman-Tobias-Klein barostat
pcoupltype = isotropic ; uniform scaling of box vectors
tau-p = 2.0 2.0 2.0 2.0 ; time constant, in ps
ref-p = 1.0 1.0 1.0 1.0 ; reference pressure, in bar
compressibility = 5.2e-5 ; isothermal compressibility of water, bar^{-1}
refcoord-scaling = com
; Periodic boundary conditions
pbc = xyz ; 3-D PBC
;periodic-molecules=yes
; Dispersion correction
DispCorr = EnerPres ; account for cut-off vdW scheme
; Velocity generation
gen-vel = yes ; Velocity generation is on
gen-temp = 310 ; temperature for Maxwell distribution
gen-seed = -1 ; generate a random seed

Bibliography

[1] Agnieszka Z. Wilczewska, Katarzyna Niemirowicz, Karolina H. Markiewicz. *Nanoparticles as drug delivery systems.* Pharmacological Reports. 2012, 64, 1020-1037.

[2] Devarajan PV, Sonavane GS, Doble M (2005) Computer-aided molecular modeling: a predictive approach in the design of nano-particulate drug delivery system. J Biomed Nanotechnol 1:1–9

[3] National Cancer Institude Fact Sheet
www.cancer.gov/cancertopics/factsheet/Therapy/targeted Last accessed: 11/10/2014

[4] Hilder TA, Hill JM (2008) *Probability of encapsulation of paclitaxel and doxorubicin into carbon nanotubes*. Micro. Nano. Lett.3:41–49

[5] Cheng, Y.; Pei, Q. X.; Gao, H.(2009) *Molecular-dynamics studies of competitive replacement in peptide–nanotubeassembly for control of drug release* Nanotechnology, 20 (14),145101

[6] Chaban VV, Savchenko TI, Kovalenko SM, Prezhdo OV (2010) *Heat-driven release of a drug molecule from carbon nanotubes: a molecular dynamics study.* J Phys Chem B 114:13481–13486

[7] Hilder, T. A.; Hill, J. M. Small (2009) *Modeling the loading and unloading of drugs into nanotubes*, 5 (3), 300–8

[8] C. F. Lopez et al (2004) *Understanding nature's design for a nanosyringe*, Proceedings of the National Academy of Sciences of the United States of America, vol. 101, no. 13, pp. 4431–4434.

[9] E. J. Wallace and M. S. P. Sansom (2008), *Blocking of carbon nanotube based nanoinjectors by lipids: a simulation study,* Nano Letters, vol. 8, no. 9, pp. 2751–2756.

[10] Capaldi FM, Gangupomu VK,(2011) *Interactions of carbon nanotube with lipid bilayer membranes.* J NanoMat 2011:6

[11] Hamid Modarrres et. al. (2013) *Carbon Nanotube-Encapsulated Drug Penetration Through the Cell Membrane: An Investigation Based on Steered Molecular Dynamics Simulation.* Journal of Membrane Biology 246:697–704 doi:10.1007/s00232-013-9587-y America, vol. 101, no. 13, pp. 4431–4434, 2004.

[12] Guven A, Rusakova A, Lewis MT, Wilson LJ.l (2012) *Cisplatin@US-tube carbon nanocapsules for enhanced chemotherapeutic delivery.* Biomaterials. 2012 Feb;33(5):1455-61. doi: 10.1016/j.biomaterials.2011.10.060. Epub 2011 Nov 12.

[13] Zhang LW1, Zeng L, Barron AR, Monteiro-Riviere NA *Biological interactions of functionalized single-wall carbon nanotubes in human epidermal keratinocytes*, Int J Toxicol. 2007 Mar-Apr;26(2):103-13; doi: 10.1063/1.1736034.

[14] Liu, Z.; Davis, C.; Cai, W.; He, L.; Chen, X.; Dai, H.
Circulation and long-term fate of functionalized, biocompatible single-walled carbon nanotubes in mice probed by Raman spectroscopy Proc Natl Acad Sci U S A. 2008 Feb 5;105(5):1410-5. doi: 10.1073/pnas.0707654105. Epub 2008 Jan 29.

[15] Allen, M. P., and Tildesley, D. J., (1986). *Computer Simulation of Liquids.* Oxford: Clarendon Press p230.

[16] Yanxiang zhao *Brief introduction to the thermostats*
http://www.math.ucsd.edu/ y1zhao/Resources.html. Last accessed: 05/12/2014

[17] Dann Frenkel, Berend Smit (2002) *Understanding Molecular Simulation: From Algorithms to Application*, Academic Press, 2002.

[18] Alan Hinchliffe. (2003) *Molecular Modelling for Beginners.* West Sussex, England. John Wiley & Sons Ltd. p135

[19] Berendsen, H. J. C.; Postma, J. P. M.; van Gunsteren, W. F.; DiNola, A.; *Molecular dynamics with coupling to an external bath* The Journal of Chemical Physics 81 (1984) 3684

[20] Morishita, T.*Fluctuation formulas in molecular-dynamics simulations with the weak coupling heat bath* The Journal of Chemical Phys 113 (2000) 2976–2982. doi:10.1063/1.1287333

[21] http://www.gromacs.org Last accessed: 09/12/2014.

[22] Humphrey, W., Dalke, A. and Schulten, K.,(1996) *VMD - Visual Molecular Dynamics*, J. Molec. Graphics, 14.1, 33-38.

[23] Berendsen HJC, Postma JPM, van Gunsteren WF, Hermans J (1981)*Interaction models for water in relation to protein hydration.* Intermolecular Forces,The Jerusalem Symposia on Quantum Chemistry and Biochemistr 14, 1981, pp 331-342.

[24] W. L. Jorgensen, D. S. Maxwell, and J. Tirado-Rives (1996) J. Am. Chem. Soc. 118 (45): 11225-11236. DOI: 10.1021/ja9621760

[25] Wallace EJ, Sansom MSP (2008) *Blocking of carbon nanotube based nanoinjectors by lipids: a simulation study.* Nano Lett 8:2751–2756

[26] http://people.ucalgary.ca/ tieleman/download.html Last accessed: 24/11/2014

[27] Berger, O.; Edholm, O.; Jahnig, F. (1997) *Molecular Dynamics Simulations of a Fluid Bilayer of Dipalmitoylphosphatidylcholine at Full Hydration, Constant Pressure, and Constant Temperature.* Biophys. J. , 72, 2002−2013.

[28] Panczyk T, Warzocha P, Camp PJ (2010) *A magnetically controlled molecular nanocontainer as a drug delivery system: the effects of carbon nanotube and magnetic nanoparticle parameters from Monte Carlo simulations.* J Phys Chem C 114:21299–21308

[29] LaVan DA, McGuire T, Langer R (2003) *Small-scale systems for in vivo drug delivery.* Nat Biotechnol 21:1184–1191

[30] Yong Zhao, Brett L. Allen, and Alexander S.(2011) *Enzymatic Degradation of Multiwalled Carbon Nanotubes*J. Phys. Chem. A, 115 (34), pp 9536–9544 DOI:10.1021/jp112324d

[31] H.J.C. Berendsen, J.P.M. Postma, W.F. van Gunsterne, A. DiNola, J.R.Haak,(1984) *Molecular dynamics with coupling to an external bath*, J Chem. Phy. 81, 3684 (1984); doi: 10.1063/1.448118 and Physics Communications, 2008.01.006

[32] H.C. Anderson,(1980) *Molecular dynamics simulations at constant pressure and/or temperature*, J. Chem. Phys, 72(4).

[33] S.J. Marrink, O. Berger, D.P. Tieleman, F. Jaehnig (1998) *Adhesion forces of lipids in a phospholipid membrane studied by molecular dynamics simulations* , Biophys. J. 74, pp. 931-943

[34] Martyna, G. J., Tuckerman, M. E., Tobias, D. J., Klein, M. L. (1996) *Explicit reversible integrators for extended systems dynamics.* Mol. Phys. 87:1117–1157.

[35] Nose, S (1984). *A unified formulation of the constant temperature molecular-dynamics methods*, Journal of chemical physics 81 (1): 511–519. doi:10.1063/1.447334

[36] Hoover,W. G. (1985) *Canonical dynamics: Equilibrium phase-space distributions*, Phys. Rev. A 31 (3): 1695–1697. doi:10.1103/PhysRevA.31.1695

[37] Kostas Kostarelos et al. (2007) *Cellular uptake of functionalized carbon nanotubes is independent of functional group and cell type* Nature Nanotechnology 2, 108 - 113 (2007) doi:10.1038/nnano.2006.209

[38] Zhang LW, Zeng L, Barron AR and Monteiro-Riviere, N. (2007) *Biological interactions of functionalized single-wall carbon nanotubes in human epidermal keratinocytes.* Int J Toxicol. 2007 Mar-Apr;26(2):103-13.

[39] Pantarotto D, Briand JP, Prato M, Bianco A. (2004) *Translocation of bioactive peptides across cell membranes by carbon nanotubes*,Chem. Commun. 1, 16–17 .

[40] Cherukuri P, Bachilo SM, Litovsky SH, Weisman RB.(2004) *Near-infrared fluorescence microscopy of single-walled carbon nanotubes in phagocytic cells*, J. Am. Chem. Soc. 126, 15638–15639

[41] Lara Lacerdaa, Simona Raffab, Maurizio Pratoc, Alberto Biancod, Kostas Kostarelosa (2007) *Cell-penetrating CNTs for Delivery of Therapeutics*. Nano Today 2(6).